Colloid Polym Sci (2010) 288:1435–1444
DOI 10.1007/s00396-010-2281-z

ORIGINAL CONTRIBUTION

Dissipative crystallization of sodium salt of deoxyribonucleic acid

Tsuneo Okubo · Masashi Mizutani · Shinya Takahashi · Akira Tsuchida

Received: 27 June 2010 / Revised: 23 July 2010 / Accepted: 8 August 2010 / Published online: 24 August 2010

Abstract Drying patterns of aqueous solutions of sodium salt of deoxyribonucleic acid (NaDNA) were studied on a cover glass, a watch glass, and a Petri glass dish at room temperature. Orientation of the rod-like single crystals of NaDNA molecules in the radial direction was observed especially at low polymer concentrations. The ratios of the size of the broad ring against initial size of the liquid on a cover glass and a watch glass were very small between 0.05 and 0.1 compared with those of the typical polyelectrolytes. Main cause is the compact conformation of NaDNA forming single or double stranded helix structures in the dried film. Microscopic drying patterns were long rods accompanied with the many short rods especially on a cover glass. Thick and short rods and dendritic crystals were fogrmed at the inward and outward areas of the dried films, respectively, on a watch glass and a Petri glass dish. Rod-like and dendritic crystals resembled the distorted hedrite and/or spherulite structures. Dissipative crystallization such as the orientation and accumulation of the single crystals of NaDNA were observed and the importance of the convectional and sedimentation processes was demonstrated during the course of crystallization.

T. Okubo (✉) · A. Tsuchida
Institute for Colloidal Organization,
Hatoyama 3-1-112, Uji, Kyoto 611-0012, Japan
e-mail: okubotsu@ybb.ne.jp

M. Mizutani · S. Takahashi · A. Tsuchida
Department of Applied Chemistry, Faculty of Engineering,
Gifu University,
Gifu 501-1193, Japan

Keywords Drying dissipative structure · Dissipative crystallization · Sodium salt of deoxyribonucleic acid (NaDNA) · Orientation of rods

Introduction

Most structural patterns in nature form via self-organization accompanied with the dissipation of free energy and in the non-equilibrium state. In order to understand the mechanisms of the dissipative self-organization of the simple model systems, instead of the much complex nature itself, the authors have studied the convectional, sedimentary, and drying dissipative patterns during dryness of colloidal suspensions and solutions as systematically as possible, though these three kinds of structures are correlated strongly and overlapped to each other [1–3]. Furthermore, studies on the drying patterns of colloidal suspensions and polymer solutions are highly important in the industrial aspects such as painting, printing, and micro-array device fields.

Typical convectional patterns are Benard cell [4, 5], the hexagonal circulating pattern and Terada cell [6–8], the spoke-lines spreading whole the liquid surface accompanied with the huge number of cell convections in the normal direction of the spoke lines. These convectional patterns were observed often with the naked eyes in the intermediate and final steps in the convectional processes [9–17]. Recently, the whole processes of the convectional patterns have been clarified experimentally [11, 13, 14]. Theoretical studies of the convectional patterns have been reported mainly using Navier–Stokes equations [18–23]. However, these are not always successful yet when the theories are compared with the experiments.

Sedimentary dissipative patterns during the course of drying suspensions have been studied in detail on a cover glass, a watch glass, a glass dish and others, for the first time, in our laboratory [11, 24–31]. The broad ring-like patterns were formed in suspension state. It was clarified that the sedimentary particles were suspended above the substrate by the electrical double layers around the particles and always moved by the balancing of the force fields between the convectional flow and the gravitational sedimentation. Quite recently, dynamic bundle-like sedimentary patterns formed cooperatively from the spoke-like convectional structures of coffee [13] and black tea [14] coexisted with cream.

Drying dissipative patterns have been studied for many kinds of colloidal particles [9, 10, 13–17, 24–49], linear-type synthetic and bio-polyelectrolytes [50–52], water-soluble neutral polymers [53, 54], ionic and non-ionic detergents [40, 55, 56], gels [57], colloidal polymer complex [58], and dyes [59]. The macroscopic broad ring patterns of the hill accumulated with the solutes formed. The broad rings moved inward when solute concentration decreased and/or solute size increased. For the non-spherical particles, the round hill was formed in the central area in addition to the faint broad ring. Macroscopic spoke-like cracks or fine hills including flickering spoke-like ones were also observed for many solutes. Beautiful fractal patterns such as branch-like, arc-like, block-like, star-like, cross-like, and string-like ones were observed in the microscopic scale.

One of the important findings in our experiments is that the primitive vague sedimentary patterns were formed already in the concentrated suspensions or solutions before dryness and they grew toward fine structures in the processes of the solidification. It has been also clarified that information of the suspensions and solutions, shape and size of solute and atmospheric humidity and temperature, for example, is transferred into the drying patterns. Furthermore, dissipative crystallization of poly (allylamine hydrochloride) [49], poly (ethylene glycol) [60], sodium salt of poly (methacrylic acid) [61], poly-D-lysine and poly-L-lysine hydrobromides [62], and hydroxypropyl cellulose [63] has been studied in detail. Accumulation, uneven distribution, symmetric distribution, and ordering of the polymer single crystals, and further coupling of the single crystals with the dissipative broad ring patterns have been clarified.

In this work, the drying dissipative structures of NaDNA in aqueous solution are studied in detail. NaDNA is one of the convenient polymers for studying the dissipative effects such as orientation and accumulation of the single crystals in the drying processes, since the anisotropic shaped single crystals such as rod-like and dendritic structures are formed in the dried film on the various substrates, where the convectional and sedimentary effects play an important role during the course of dryness of the solution.

Experimental

Materials

Sodium salt of deoxyribonucleic acid (NaDNA, Lot No. 6078C) was purchased from MP Biochemicals, Inc. (Solon, OH, USA). The aqueous solution of NaDNA at 0.01 monoM was filtrated in order to delete a slight amount of the contaminated dust, and the stock solution was obtained. A standard solution of sodium chloride at 0.1 M was purchased from Wako Pure Chemical Industries, Ltd. (Osaka, Japan). The water used for the sample preparation was purified by a Milli-Q reagent grade system (Advantage A10, Millipore, Bedford, MA, USA).

Observation of the dissipative structures

Of the solution, 0.1 mL was dropped carefully and gently on a micro-cover glass (30 mm×30 mm, thickness No.1, 0.12–0.17 mm, Matsunami Glass Co., Kishiwada, Osaka) set in a plastic dish (type NH-52, 52 mm in diameter, 8 mm in depth, As One Co., Tokyo). The cover glasses were used without further rinse. The contact angle of the pure water was 31±0.5° from the drop profiles of water on an unrinsed cover glass. Extrapolation to the zero amount of water was made from the measurements at the several amount of water. Of the solution, 4.0 mL was set on a watch glass (70 mm in diameter, Toshinriko Co. TOSTK-70, Tokyo); 5.0 mL was put into a Petri glass dish (46.5 mm in outer diameter and 18 mm in height, TOP Co., code 305-02). The disposable serological pipets (1.0 ml, 5.0 ml and 10 ml, Codes 7077-1 N, 7077-5 N, and 7077-10 N, Corning Lab. Sci., CO, USA) were used for the preparation and setting solutions. Observation of the macroscopic and microscopic patterns was made in an air-conditioned room at 25 °C and 45–55% in humidity.

Macroscopic close-up pictures were taken on a Canon EOS 10D camera with a macro-lens (EF 50 mm, f=2.5) plus a life-size converter EF. Microscopic patterns were observed with a metallurgical microscope (PME-3, Olympus Co., Tokyo). Polarizing microscopic pictures were taken on a Shimadzu polarizing microscope (type Kalnew 53255, Shimadzu, Kyoto) with a CCD camera (type TNC4604J, Kenis Ltd., Osaka). Thickness profiles of the dried films on a cover glass were made on a laser 3D profile microscope (type VK-8500, Keyence Co., Osaka, Japan).

Evaluation of the sloping angle and the orientation index

In order to study the orientation effect of the main rods of NaDNA molecules in the dried films, the sloping angles of all the main rods in a macroscopic picture from the radial direction were measured. The mean values of sloping angle (θ; $0<\theta<90°$) and their standard deviations were evaluated for each macroscopic pictures. Thus, the θ value is one of the typical parameters showing the orientation of the main rods from the radial direction (θ~0°) to the ring direction (θ~90°). The orientation indices (*o.i.*) were also evaluated, where the sloping angles with plus or minus signs depending on the right-hand side or left-hand side deviations from the radial direction, respectively, were averaged. The orientation index shows the averaged deviation among all the main rods observed in a macroscopic picture.

Table 1 Sloping angle (θ) and the orientation index (*o.i.*) of the crystal rods from the radial direction

[NaDNA]	[NaCl]	Cover glass		Watch glass	
(monoM)	(M)	θ (degree)	*o.i.*	θ (degree)	*o.i.*
0.01	0	71±11	−23	34±10	+21
0.0067	0	50±11	−16	40±12	+1.8
0.005	0	50±14	−4	75±7	−15
0.0033	0	15±5	+5	42±11	−20
0.002	0	25±5	−11	49±16	+4
0.001	0	22±5	−3	45±12	+2
0.005	0	70±11	−28	47±14	−7
0.005	0.002	53±10	−28	21±7	+4
0.005	0.01	38±12	−13	31±10	+11
0.005	0.0333	–	–	20±7	+2
0.005	0.1	–	–	12±4	+2
0.005	0.2	14±9	+1.4	10±4	−0.5

Results and discussion

Macroscopic drying patterns of NaDNA

Figure 1 shows the typical examples of the macroscopic drying patterns on a cover glass. Concentrations of NaDNA range from 0.001 monoM to 0.01 monoM. Long rod-like single crystals accompanied with the many but short rods grown from the main rod with a right angle were packed densely within the broad ring area at the outside edge. Interestingly, the long rods were arrayed in the radial direction especially at low polymer concentrations. The rods were oriented in the monolayer state on the substrate and not piled up in most cases. Table 1 shows the mean absolute values of the θ of the main rods from the radial direction and the *o.i.*, which show the mean values of the slope angles including their directions (right-hand side and left-hand side deviations from the radial direction are given by the angles with plus and minus signs, respectively). Clearly, the θ values decreased sharply as the polymer concentration decreased on a cover glass as is shown in the table. The growing of the rod-like single crystals takes place under the convectional flow of water in the radial direction [11, 13, 14]. Main cause for the concentration dependency of the orientation is the difficulty in the orientation of the very long rods along the

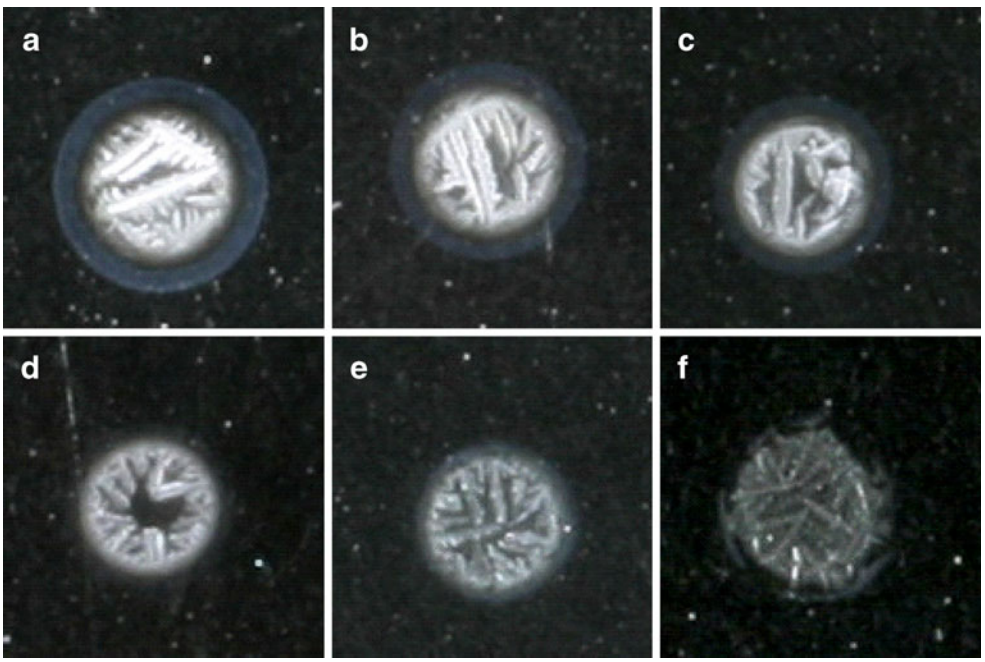

Fig. 1 Macroscopic drying patterns of NaDNA on a cover glass at 25 °C.
a [NaDNA]=0.01 monoM,
b 0.0067 monoM,
c 0.005 monoM,
d 0.0033 monoM,
e 0.002 monoM,
f 0.001 monoM

radial direction at the high polymer concentrations. At low concentrations, the rod-like single crystals became short and the orientation took place much easier. Figure 2 shows the macroscopic drying patterns on a watch glass. The θ values were quite insensitive to the polymer concentration, which is contrast with the concentration dependency of θ values on a cover glass as is shown in Table 1. This is due to the fact that the length of the main rods was not sensitive to the initial polymer concentration as is shown in Fig. 2.

Figure 3a shows the ratios of the sizes of the broad rings (d_f) against those of the initial solutions (d_i). Surprisingly, the ratios were very small between 0.05 and 0.1, which clearly indicates that the excluded volume of each DNA molecule is quite small compared with the total volume of the initial solution. The d_f/d_i values of the several other polyelectrolytes were much large and even close to unity [50, 61, 62], which was clearly due to the very large excluded volumes of the macroions by the extended or loosely coiled rods in the absence of the foreign salts. Main cause for the small d_f/d_i values of NaDNA, on the other hand, is due to the fact that they form the compact single- or double-stranded helix structures in solution. The d_f/d_i values decreased as polymer concentration decreased and turned to increase with further dilution as is shown in the figure. Decreasing tendency of the d_f/d_i values with decreasing concentration has been observed so often for many solutions and suspensions hitherto [15–17, 28, 29, 40, 49, 60]. Main cause for the increase of the broad ring size with decreasing concentration at the low polymer concentrations is not clear, but it is highly plausible that the extention of the conformation of the DNA molecules and then the increase in the excluded volumes of the polyelectrolytes. It should be noted here that the concentration dependency of the broad ring size does not support

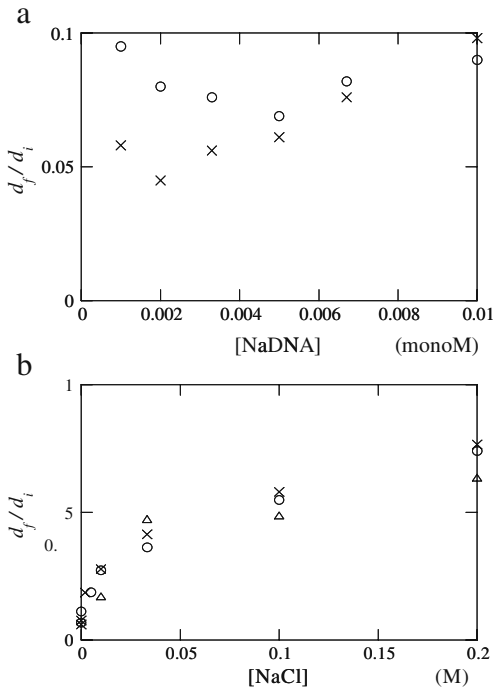

Fig. 3 **a** d_f/d_i of NaDNA as a function of polymer concentration at 25 °C. **b** d_f/d_i of NaDNA as a function of NaCl concentration at 25 °C; [NaDNA]=0.005 monoM

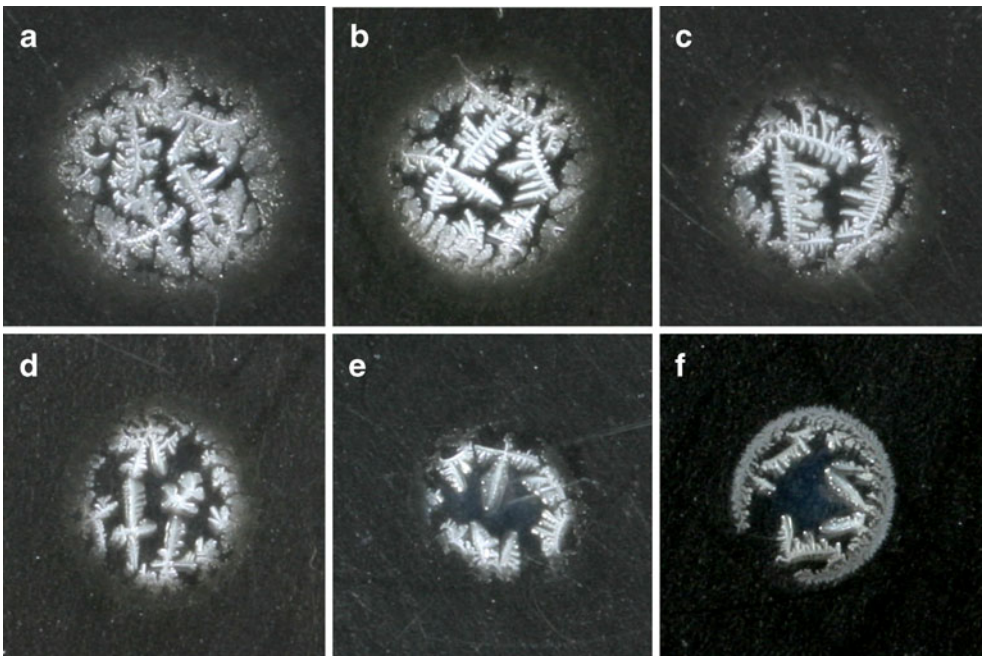

Fig. 2 Macroscopic drying patterns of NaDNA on a watch glass at 25 °C.
a [NaDNA]=0.01 monoM,
b 0.0067 monoM,
c 0.005 monoM,
d 0.0033 monoM,
e 0.002 monoM,
f 0.001 monoM

the pinning effect of the contact line proposed by Deegan et al. [22], where the contact line should keep at the outside edge of the initial solution.

Figure 4 shows typical examples of the drying patterns of NaDNA solutions in the presence of sodium chloride on a cover glass. Bluish and whitey broad rings appeared and their sizes increased sharply as the salt concentration increased. Main composition of the whitey broad ring is sodium chloride. Bluish ring structures were faint and recognized even in the absence of the salt as is seen in Fig. 4a. It is highly plausible that the main compositions of the bluish rings are low molecular weight analogs of DNA molecules contaminated in the samples. It should be recalled that the size of the broad ring is very sensitive to the molecular weights of solutes, colloidal size and/or concentration of solutes, and increased as these parameters increased [1–3]. Furthermore, segregation effects in the drying patterns of the binary and ternary solute mixtures have been observed with high-resolution efficiency, i.e., (1) broad rings originated from the low and high molecular weights were segregated at the outward and inward areas [28, 29]. (2) Salt and polymer (or colloidal) solutes were segregated outward and inward, respectively [24–26, 46, 48, 52, 64]. Interestingly, the cooperative complexations of DNA molecules with NaCl ions were observed at the broad ring areas and the inner regions from the broad ring area. In both areas, the rod-like DNA crystals were oriented around the single crystals of NaCl. It should be noted here that the cooperated drying patterns were also observed for colloidal silica suspensions with sodium chloride, where the cross-like structure of NaCl was surrounded cooperatively by the dendritic-arranged silica spheres in a glass dish [25].

On a watch glass, the drying patterns were similar to those on a cover glass as is shown in Fig. 5. The cooperative complexation between NaDNA and NaCl are clear especially in the inner area of the broad ring. Figure 6 shows the drying patterns of NaDNA+NaCl in a Petri glass dish. The broad ring size increased as concentration of NaCl increased, though the assignment of the main broad ring was not easy in part. The d_f/d_i values of the NaDNA+NaCl systems on a cover glass, a watch glass, and a Petri glass dish are displayed in Fig. 3b. The ratios increased as salt concentration increased and were insensitive to the cells used.

The orientation effects of the rods in the presence of NaCl are compiled in Table 1. The θ values decreased on a cover glass and a watch glass when the salt concentration increased. The main cause is clearly due to the increasing drying area with increasing salt concentration. It should be noted here that the experimental errors of the θ and *o.i.* parameters were rather large. For example, the observed values of θ at the same experimental condition but at independent experiments at different days were 50±14 and 70±11 on a cover glass and 75±7 and 47±14 on a watch glass, respectively, as is shown in Table 1.

Microscopic drying patterns of NaDNA

Figure 7a and b show the microscopic drying patterns on a cover glass and a watch glass. On a cover glass, most

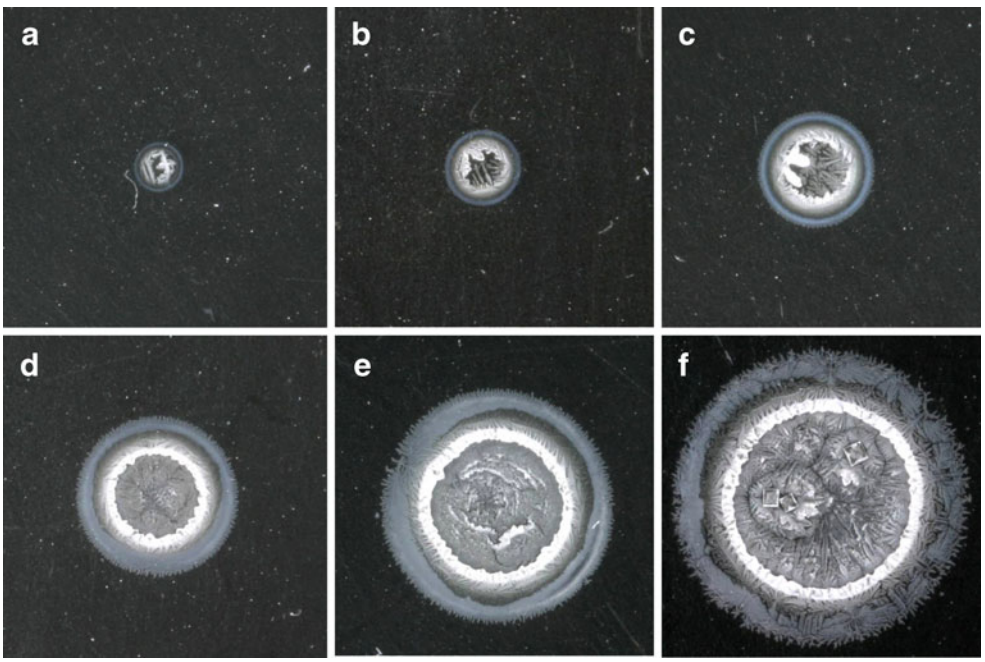

Fig. 4 Macroscopic drying patterns of NaDNA on a cover glass at 25 °C. [NaDNA]=0.005 monoM, **a** [NaCl]=0 M, **b** 0.002 M, **c** 0.01 M, **d** 0.033 M, **e** 0.1 M, **f** 0.2 M

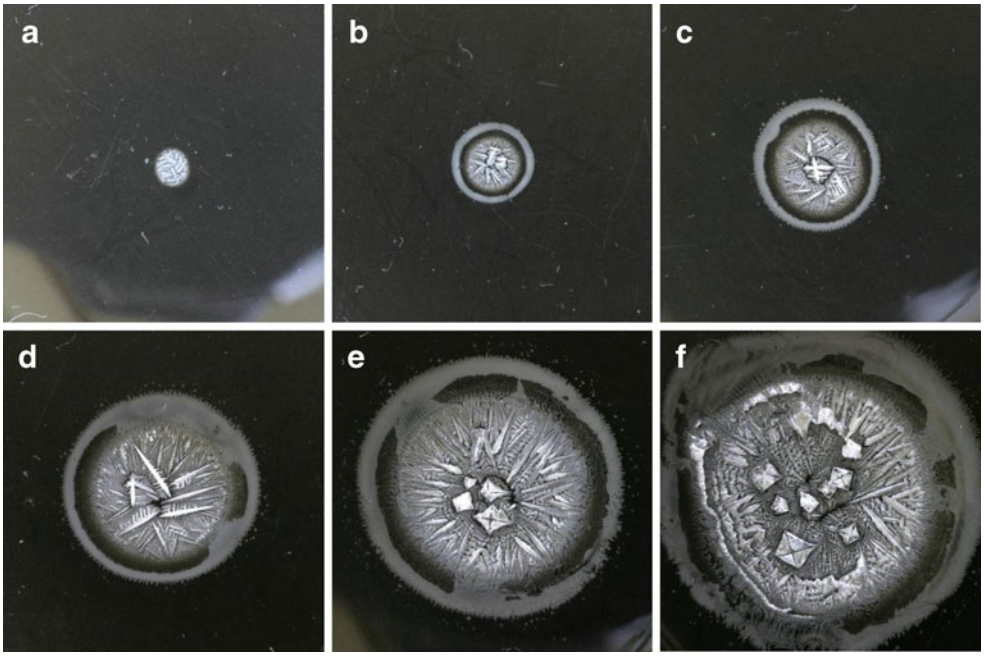

Fig. 5 Macroscopic drying patterns of NaDNA on a watch glass at 25 °C. [NaDNA]=0.005 monoM, **a** [NaCl]=0 M, **b** 0.002 M, **c** 0.01 M, **d** 0.033 M, **e** 0.1 M, **f** 0.2 M

single crystals were long rods accompanied with the many and short rods. Very small block-like single crystals were also distributed in the vacant spaces between the rods. Outside edges of the broad ring areas, very small dendritic single crystals were observed especially at the high polymer concentrations. On the other hand, on a watch glass dendritic crystals were grown up at the much wide areas of the outside regions of the dried films, whereas the jointed thick and short rods were observed in the central area (see Fig. 7b). It should be noted here that both the dendritic and thick rod crystals look quite similar to the distorted hedrite structures, primitive structure of the spherulite. Polarizing microscopic observation did not show clear-cut maltese-cross patterns. However, light and dark changes of the crystallites were recognized clearly when the drying samples were rotated slowly. It should be noted here that NaDNA solutions especially at high polymer

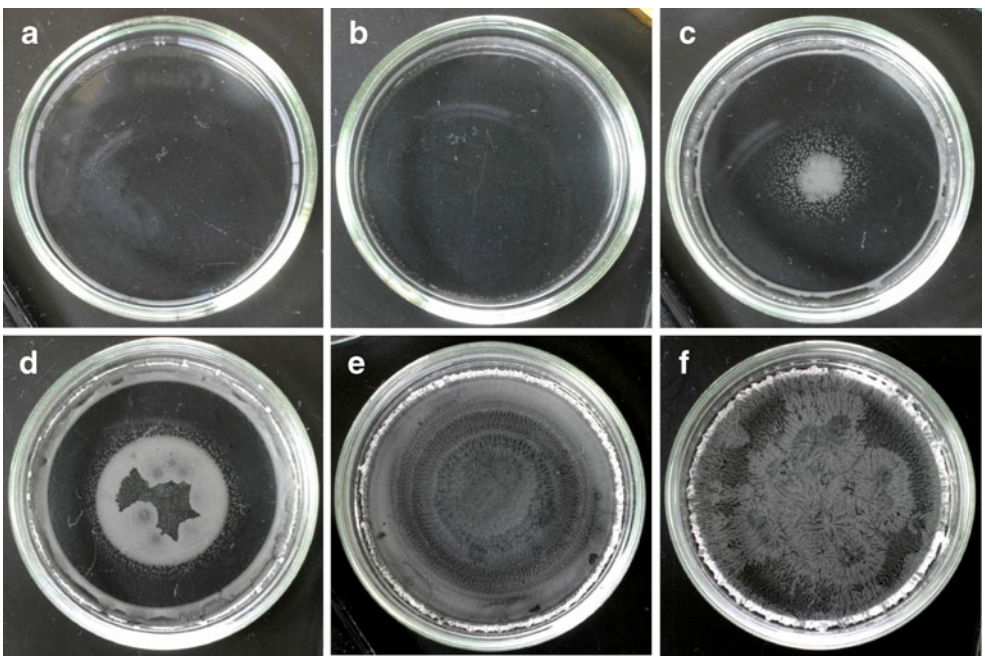

Fig. 6 Macroscopic drying patterns of NaDNA on a Petri glass dish at 25 °C. [NaDNA]=0.005 monoM, **a** [NaCl]=0 M, **b** 0.002 M, **c** 0.01 M, **d** 0.033 M, **e** 0.1 M, **f** 0.2 M

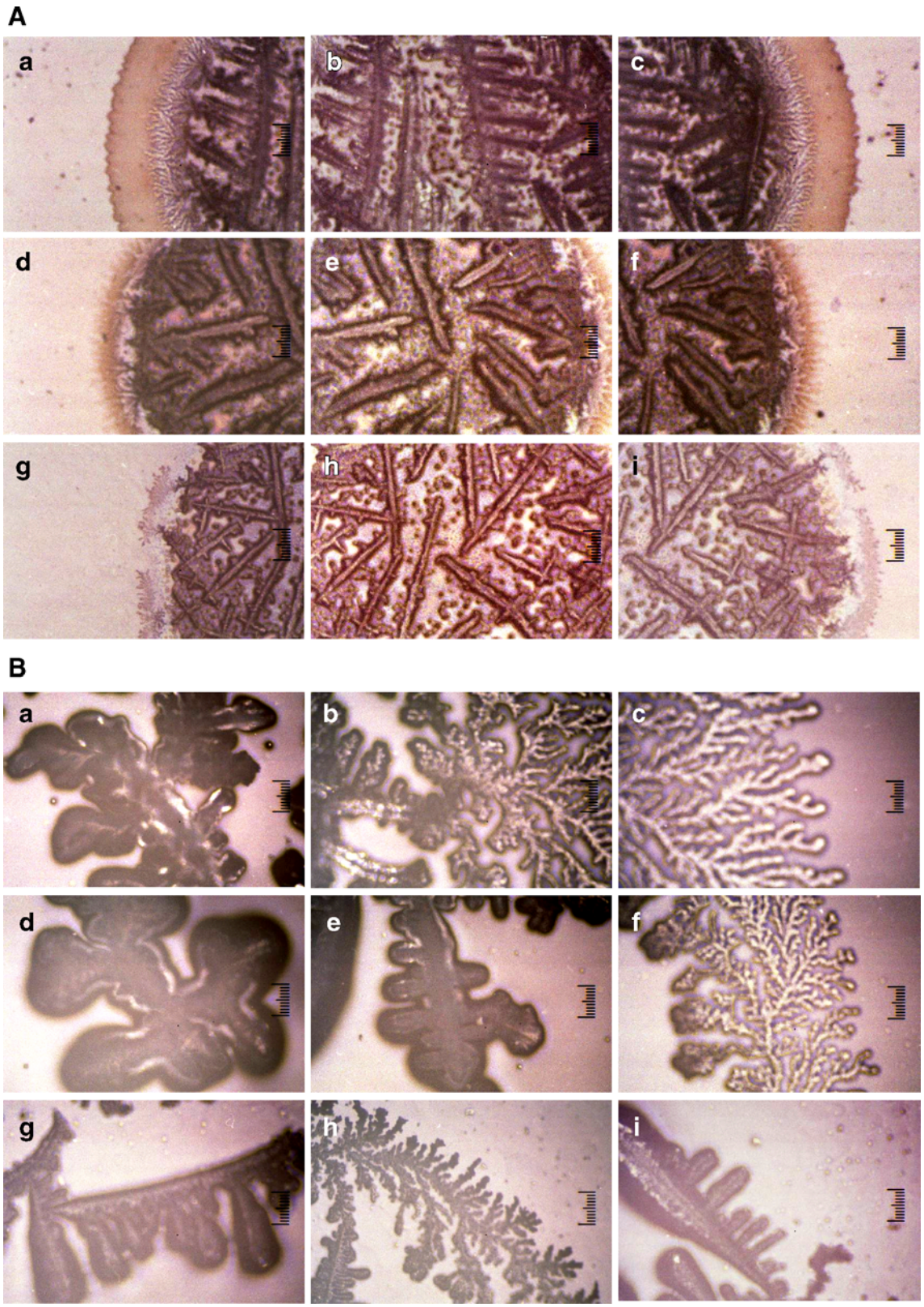

Fig. 7 **a** Microscopic drying patterns of NaDNA on a cover glass at 25 °C. *a–c* [NaDNA]=0.01 monoM, *d–f* 0.002 monoM, *g–i* 0.001 monoM, *a*, *d*, *g* to *c*, *f*, *i* from the left edge to the right in the central area, full scale is 100 μm. **b** Microscopic drying patterns of NaDNA on a watch glass at 25 °C. *a–c* [NaDNA]=0.01 monoM, *d–f* 0.0033 monoM, *g–i* 0.001 monoM, *a*, *d*, *g* to *c*, *f*, *i* from the center to the right edge in the central area, full scale is 100 μm

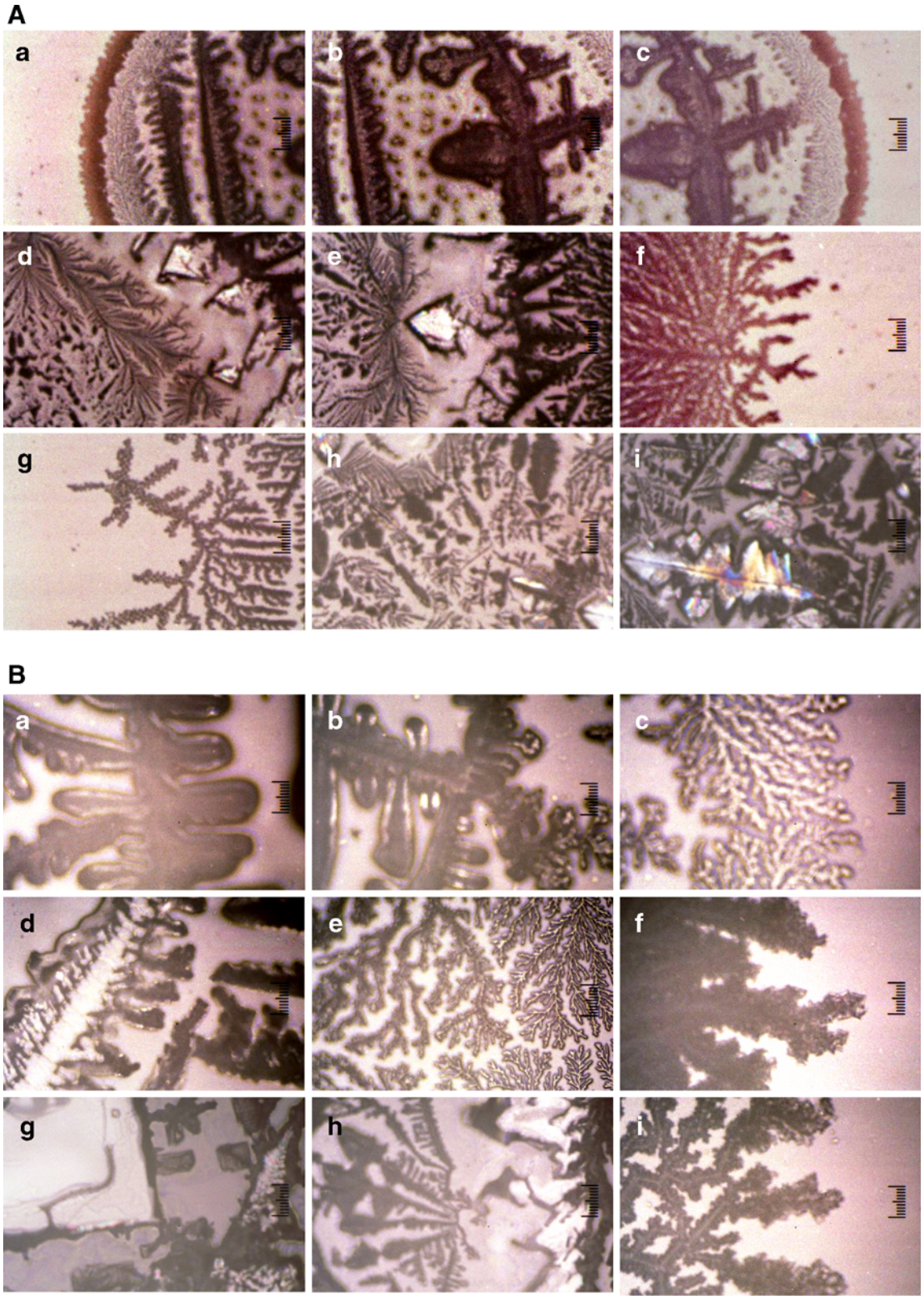

Fig. 8 **a** Microscopic drying patterns of NaDNA on a cover glass at 25 °C. [NaDNA]=0.005 monoM, *a–c* [NaCl]=0 M, *d–f* 0.0333 M, *g–i* 0.2 M, *a* to *c* from the left edge to the right, *d* to *f* from the center to the right edge, *g* to *i* from the left edge to the center, full scale is 100 μm. **b** Microscopic drying patterns of NaDNA on a watch glass at 25 °C. [NaDNA]=0.005 monoM, *a–c* [NaCl]=0 M, *d–f* 0.0333 M, *g–i* 0.2 M, *a*, *d*, *g* to *c*, *f*, *i* from the center to the right edge, full scale is 100 μm. **c** Microscopic drying patterns of NaDNA on a Petri glass dish at 25 °C. [NaDNA]=0.005 monoM, *a–c* [NaCl]=0.002 M, *d–f* 0.0333 M, *g–i* 0.2 M, *a*, *d*, *g* to *c*, *f*, *i* from the center to the right edge, full scale is 100 μm

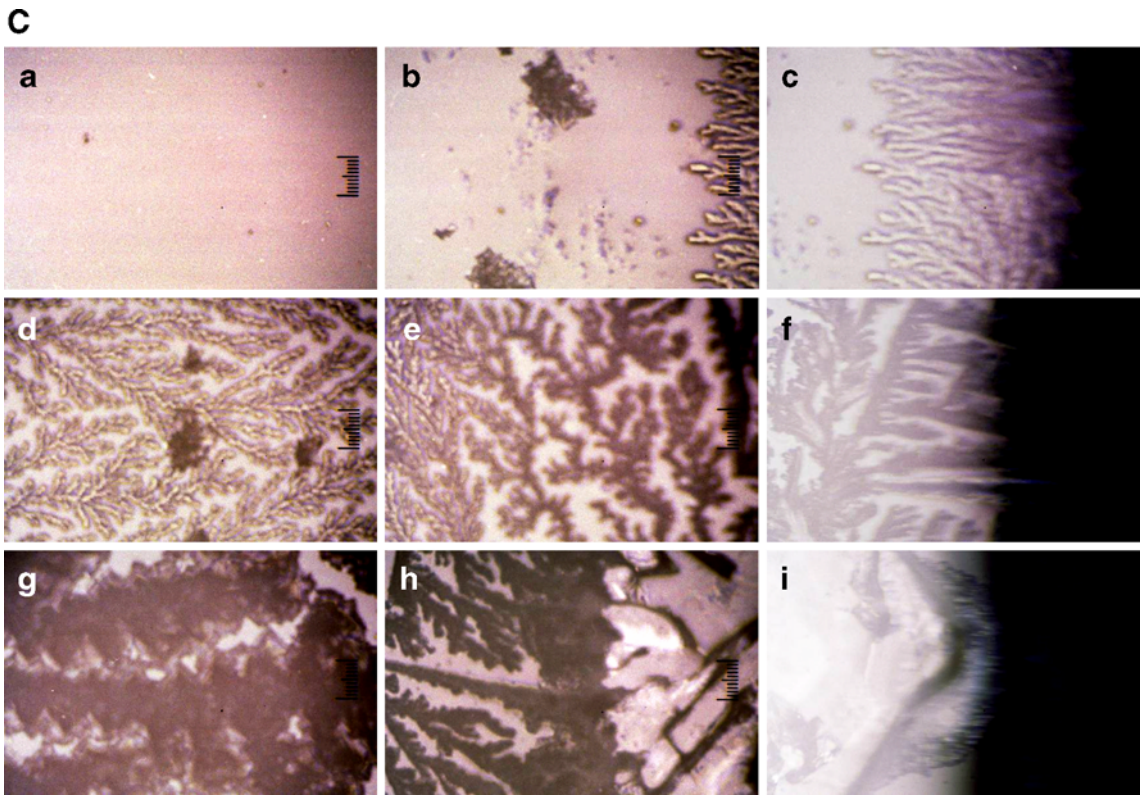

Fig. 8 (continued)

concentrations form liquid–crystalline phases and form rod-like assemblies [65–67].

Figure 8a–c show the microscopic patterns demonstrating salt effects on the morphologies of the single crystals of NaDNA molecules on a cover glass, a watch glass and a Petri glass dish, respectively. By the addition of sodium chloride, microscopic patterns showing the cooperative complexation between NaDNA and NaCl were observed in some places (see e and i of Fig. 8a, d and i of Fig. 8b, and g of Fig. 8c, for example). In most cases, block-like or rod-arrayed crystals of NaCl was surrounded by the arrayed NaDNA rods or dendrites cooperatively.

Concluding remarks

Several kinds of dissipative polymer crystallization such as the orientation and/or broad ring-like accumulation of the rod-like crystallites were observed in this study. Clearly, morphologies of single crystals of NaDNA in the dried film have been influenced greatly by the successive and dissipative processes of convection, sedimentation, and solidification during dryness. Among the many processes, the convectional flow steps will be most important for the orientation of the single crystals in the dried film. The spoke-like flow shown by Benard cell [4, 5] and Terada cell [6–8] and the large number of cell convections of the Terada cell must be the main origin for the radial orientations of the rod-like single crystals of NaDNA molecules. It should be mentioned here that the morphologies of NaDNA crystals were also influenced strongly by the dissipative processes of convection, sedimentation and solidification. Conformational information of poly (allylamine hydrochloride) in the initial aqueous solution was transferred to the microscopic drying patterns of crystals [50]. Symmetrical ordering of the polymer single crystals and further coupling of the spherulites and the lamellae originated from the broad ring patterns were observed during dryness of aqueous solution of poly (ethylene glycol) [60] and sodium salts of poly (methacrylic acid) [61]. Shape and size of the single crystals of polylysine hydrobromide changed greatly as a function of the distance from the center of the drying film [62, 63]. Several important factors causing the dissipative crystallization are proposed from the authors' work hitherto; (1) thermal movement of solutes and solvents, (1) solute–solute and solute–substrate (cell wall) interaction, (3) gravitational and Marangoni convection of solvents and solutes, (4) sedimentation of solutes, and (5) important role of the electric double layers for the colloidal suspensions.

Acknowledgments Financial supports to TO and AT from the Ministry of Education, Culture, Sports, Science and Technology, Japan and Japan Society for the Promotion of Science are greatly acknowledged for Grants-in-Aid for Exploratory Research and Scientific Research (B), respectively. Research fund from REX Co. (Tokyo) to TO is highly appreciated.

References

1. Okubo T (2006) In: Stoylov SP, Stoimenova MV (eds) Molecular and colloidal electro-optics. Taylor & Francis, New York, p 573
2. Okubo T (2008) In: Nagarajan R, Hatton TA (eds) Nanoparticles: syntheses, stabilization, passivation and functionalization. ACS Book, Washington DC, p 256
3. Okubo T (2010) Macromol Symp 288:67
4. Gribbin G (1999) Almost everyone's guide to science. The universe, life and everything. Yale University Press, New Haven
5. Ball P (1999) The self-made tapestry. Pattern formation in nature. Oxford Univ Press, Oxford
6. Terada T, Yamamoto R, Watanabe T (1934) Sci Paper Inst Phys Chem Res Jpn 27:173, Proc Imper Acad Tokyo 10:10
7. Terada T, Yamamoto R, Watanabe T (1934) Sci Paper Inst Phys Chem Res Jpn 27:75
8. Nakaya U (1947) Memoirs of Torahiko Terada (Japanese). Kobunsya, Tokyo
9. Okubo T, Kimura H, Kimura T, Hayakawa F, Shibata T, Kimura K (2005) Colloid Polym Sci 283:1
10. Okubo T (2006) Colloid Polym Sci 285:225
11. Okubo T (2009) Colloid Polym Sci 287:167
12. Deegan RD, Bakajin O, Dupont TF, Huber G, Nagel SR, Witten TA (1997) Nature 389:827
13. Okubo T, Okamoto J, Tsuchida A (2009) Colloid Polym Sci 287:351
14. Okubo T (2009) Colloid Polym Sci 287:645
15. Okubo T, Okamoto J, Tsuchida A (2008) Colloid Polym Sci 286:1123
16. Okubo T (2008) Colloid Polym Sci 286:1307
17. Okubo T (2008) Colloid Polym Sci 286:1527
18. Palmer HJ (1976) J Fluid Mech 75:487
19. Anderson DM, Davis SH (1995) Phys Fluids 7:248
20. Pouth AF, Russel WB (1998) AIChEJ 44:2088
21. Burelbach JP, Bankoff SG (1998) J Fluid Mech 195:463
22. Deegan RD, Bakajin O, Dupont TF, Huber G, Nagel SR, Witten TA (2000) Phys Rev E 62:756
23. Fischer BJ (2002) Langmuir 18:60
24. Okubo T (2006) Colloid Polym Sci 284:1191
25. Okubo T (2006) Colloid Polym Sci 284:1395
26. Okubo T, Okamoto J, Tsuchida A (2007) Colloid Polym Sci 285:967
27. Okubo T (2007) Colloid Polym Sci 285:1495
28. Okubo T, Okamoto J, Tsuchida A (2008) Colloid Polym Sci 286:385
29. Okubo T, Okamoto J, Tsuchida A (2008) Colloid Polym Sci 286:941
30. Yamaguchi T, Kimura K, Tsuchida A, Okubo T, Matsumoto M (2005) Colloid Polym Sci 283:1123
31. Okubo T (2006) Colloid Polym Sci 285:331
32. Vanderhoff JW (1973) J Polym Sci Symp 41:155
33. Nicolis G, Prigogine I (1977) Self-organization in non-equilibrium systems. Wiley, New York
34. Ohara PC, Heath JR, Gelbart WM (1997) Angew Chem 109:1120
35. Maenosono S, Dushkin CD, Saita S, Yamaguchi Y (1999) Langmuir 15:957
36. Nikoobakht B, Wang ZL, El-Sayed MA (2000) J Phys Chem 104:8635
37. Ung T, Litz-Marzan LM, Mulvaney P (2001) J Phys Chem B 105:3441
38. Okubo T, Okuda S, Kimura H (2002) Colloid Polym Sci 280:454
39. Okubo T, Kimura K, Kimura H (2002) Colloid Polym Sci 280:1001
40. Okubo T, Kanayama S, Kimura K (2004) Colloid Polym Sci 282:486
41. Okubo T, Yamada T, Kimura K, Tsuchida A (2005) Colloid Polym Sci 283:1007
42. Okubo T, Nozawa M, Tsuchida A (2007) Colloid Polym Sci 285:827
43. Okubo T, Kimura K, Tsuchida A (2007) Colloids Surf B Biointerfaces 56:201
44. Okubo T, Nakagawa N, Tsuchida A (2007) Colloid Polym Sci 285:1247
45. Okubo T, Kimura K, Tsuchida A (2008) Colloid Polym Sci 286:621
46. Okubo T (2008) Colloid Polym Sci 286:1411
47. Okubo T, Otake A, Tsuchida A (2009) Colloid Polym Sci 287:1435
48. Okubo T, Kokufuta E, Nakamuro M, Yoshinaga K, Mizutani M, Tsuchida A (2010) Colloids Surf B Biointerfaces 80:193
49. Okubo T, Suzuki H, Kitano H, Ohno K, Mizutani M, Tsuchida A (2010) Colloid Polym Sci (in press)
50. Okubo T, Kanayama S, Ogawa H, Hibino M, Kimura K (2004) Colloid Polym Sci 282:230
51. Okubo T, Onoshima D, Tsuchida A (2007) Colloid Polym Sci 285:999
52. Okubo T, Ogawa H, Tsuchida A (2010) Colloid Polym Sci 288:245
53. Shimomura M, Sawadaishi T (2001) Curr Opin Colloid Interface Sci 6:11
54. Okubo T, Yamada T, Kimura K, Tsuchida A (2006) Colloid Polym Sci 284:396
55. Kimura K, Kanayama S, Tsuchida A, Okubo T (2005) Colloid Polym Sci 283:898
56. Okubo T, Shinoda C, Kimura K, Tsuchida A (2005) Langmuir 21:9889
57. Okubo T, Itoh E, Tsuchida A, Kokufuta E (2006) Colloid Polym Sci 285:339
58. Okubo T, Okamoto J, Tsuchida A (2010) Colloid Polym Sci 288:189
59. Okubo T, Yokota N, Tsuchida A (2007) Colloid Polym Sci 285:1257
60. Okubo T, Okamoto J, Takahashi S, Tsuchida A (2009) Colloid Polym Sci 287:933
61. Okubo T, Hagiwara A, Kitano H, Okamoto J, Takahashi S, Tsuchida A (2009) Colloid Polym Sci 287:1155
62. Okubo T, Okamoto J, Tsuchida A (2010) Colloid Polym Sci 288:981
63. Okubo T, Mizutani M, Takahashi S, Tsuchida A (2010) Colloid Polym Sci (in press)
64. Okubo T, Tsuchida A, Togawa H (2009) Colloid Polym Sci 287:443
65. Iizuka E (1977) Polym J 9:173
66. Kagemoto A, Nakazaki M, Kimura S, Monohara Y, Ueno KI, Baba Y (1996) Thermochim Acta 284:309
67. Samoc A, Miniewicz A, Samoc M, Grote JG (2007) J Appl Polym Sci 105:236